https://doi.org/10.31436/iiumej.v27i1.3716

ORCA: AI-powered Autonomous Underwater Vehicle for Subaquatic Exploration

OSKAR NATAN[1]*, WIWIT SURYANTO[2], ANDI DHARMAWAN[1], RIFDA HAKIMA SARI[1], ZAIDAN HAKIM[1]

[1]*Department of Computer Science and Electronics, Universitas Gadjah Mada, Yogyakarta, Indonesia*
[2]*Department of Physics, Universitas Gadjah Mada, Yogyakarta, Indonesia*

**Corresponding author: oskarnatan@ugm.ac.id*

(Received: 1 May 2025; Accepted: 19 November 2025; Published online: 12 January 2026)

ABSTRACT: This paper presents research and development of an Autonomous Underwater Vehicle (AUV), named ORCA, to perform underwater missions independently without human intervention. ORCA plays a vital role in challenges that test robots' abilities in navigation, exploration, and interaction with the aquatic environment. Using advanced design tools, the AUV is meticulously designed in Inventor and manufactured via CNC machining, laser cutting, and 3D printing. We concentrate on the vehicle's design, manufacturing processes, control systems, PID controllers, and vision systems. Subsequently, the research and development effort is expanded to incorporate critical functionalities, including environmental perception, object detection, deep learning algorithms, and path-planning strategies. The culmination of this research has produced an AUV capable of autonomous underwater navigation, effective obstacle avoidance, efficient object detection, and precise payload manipulation using a gripper mechanism. ORCA has a comprehensive sensor suite comprising a BNO055 IMU, an MS5803-14BA pressure sensor for depth measurement, and a Logitech C525 camera for image processing. The system integration not only enhances the vehicle's operational capabilities but also represents a significant advancement in underwater robotics.

ABSTRAK: Kajian ini membentangkan penyelidikan dan pembangunan Kenderaan dalam Air Berautonomi (AUV) yang dikenali sebagai ORCA, dibangunkan bagi tujuan misi bawah air secara autonomi tanpa sebarang campur tangan manusia. ORCA memainkan peranan penting dalam menghadapi cabaran menguji kebolehan robot dalam aspek navigasi, penerokaan, serta interaksi dengan persekitaran akuatik. Dengan memanfaatkan alat reka bentuk yang canggih, AUV ini direka bentuk dengan teliti menggunakan perisian Inventor dan dihasilkan melalui teknik pemesinan CNC, pemotongan laser, dan percetakan 3D. Penekanan utama dalam penyelidikan ini adalah pada reka bentuk kenderaan, proses pembuatan, sistem kawalan, pengawal PID, serta sistem penglihatan. Selain itu, penyelidikan dan pembangunan ini turut diperluaskan bagi menyertakan fungsi-fungsi kritikal seperti persepsi persekitaran, pengesanan objek, algoritma pembelajaran mendalam, dan strategi perancangan laluan. Dapatan kajian ini telah menghasilkan AUV yang mampu melaksanakan navigasi bawah air secara autonomi, menghindari halangan dengan berkesan, mengesan objek dengan cekap, serta mengendali beban dengan tepat menggunakan mekanisme pemegang. ORCA dilengkapi dengan suit pengesan yang komprehensif, termasuk pengesan IMU BNO055, pengesan tekanan MS5803-14BA bagi pengukuran kedalaman, serta kamera Logitech C525 bagi pemprosesan visual. Integrasi sistem ini bukan sahaja meningkatkan keupayaan operasi kenderaan tetapi juga mewakili satu langkah penting dalam perkembangan robotik bawah air.

https://doi.org/10.31436/iiumej.v27i1.3716

KEYWORDS: *Robotics, Autonomous Robot Systems, Underwater Robot, Computer Vision, Navigational Control*

1. INTRODUCTION

ORCA is an Autonomous Underwater Vehicle (AUV) designed to perform independent underwater tasks without human intervention. In developing ORCA, we focus on manufacturing an Autonomous Underwater Vehicle (AUV), leveraging knowledge and experience gained in previous years and enhancing the vehicle's control systems and navigation algorithms to improve efficiency and accuracy during underwater operations. This research focuses on advancing underwater robotics by addressing challenges such as navigation in low-visibility environments, effective obstacle detection, and energy-efficient operations. ORCA aims to provide a cost-effective solution by integrating a robust mechanical design, deep learning-based vision systems, and advanced control strategies. This work leverages state-of-the-art technologies, such as pruned YOLOv8 for real-time underwater object detection and a Jetson Nano Development Kit for high-performance computing, thereby setting it apart from traditional AUV designs. Tables 1 and 2 highlight the advancements of ORCA. Key upgrades include a new single-board computer and software architecture, a transition from FreeRTOS to Ubuntu 18.04, and the incorporation of a microcontroller to assist the single-board computer with onboard computation.

Table 1. Table of Physical Specifications and Control System

Weight	Dimension	Single Board Computer	Microcontroller	Propulsion
15 kg	55cm × 70cm × 36 cm	NVidia Jetson Nano Development Kit	ESP32	8 ROVMAKER T200 Thruster

Table 2. Table of Sensor, Power, and Software Architecture Specifications

Navigation	Vision	Power Supply	Underwater Connector	Software Architecture
Sensor IMU BNO-055, Sensor MS5803-14BA	Logitech C525	14.8V 7200mAh Lipo Battery	M10, M16 Cable Penetrator, Amass XT60W and Sochi SP17H IP68 10-pin	Operating System: Ubuntu 18.04, Network Model: YOLOv8 (pruned), Deep Learning (DL) Framework: TensorFlow/Keras/Darknet, Peripherals: FPIOA, UART, GPIO, SPI, etc

This research addresses the question: How can an autonomous underwater vehicle (AUV) achieve reliable and efficient navigation, obstacle detection, and task execution in challenging underwater environments with minimal computational resources? The study explores the integration of modern hardware and software frameworks to address these challenges.

2. DESIGNS AND METHODS

2.1. Mechanical Design

The overall design of the Autonomous Underwater Vehicle (AUV), such as ORCA, must align with its research objectives, which can be categorized into two main types: high maneuverability or high speed. To achieve maneuverability, the design incorporates multiple actuators that enhance the Degree of Freedom (DoF). These actuators can be positioned at

https://doi.org/10.31436/iiumej.v27i1.3716

specific angles to direct forces as vectors, facilitating the desired movements. On the other hand, designs focused on achieving high speed prioritize a hydrodynamic shape to minimize drag forces, which the equation can express:

$$\vec{F}_{drag} = \frac{1}{2} C_d A \rho V^2 \quad (1)$$

In this equation, A represents the frontal area, ρ is the fluid density, V is the robot's speed, and C_d is the drag coefficient, which accounts for both frictional and pressure drag. The drag coefficient can be considered constant over the Reynolds number range 103–105. This assumption simplifies drag-force calculations during the design process, allowing engineers to focus on optimizing the vehicle's hydrodynamics.

2.1.1. Design Overview

Figure 1 shows the frame, which consists of various materials: a 2 mm-thick grade 430 stainless steel baseplate, 8mm-thick acrylic side panels and thruster guards, and aluminum extrusions for connections and mounts. Additionally, 3D-printed components made from PLA+ and ABS+ filament include the electronics enclosure bracket, thruster guards, and buoyancy floats. All parts are secured with stainless steel bolts and aluminum brackets. Materials were selected for their durability in underwater environments: grade 430 stainless steel and acrylic provide water resistance, while aluminum offers strength. PLA+ is chosen for its adequate strength, water resistance, and cost-effectiveness. Cost considerations were crucial in selecting materials, resulting in a high-quality yet affordable frame.

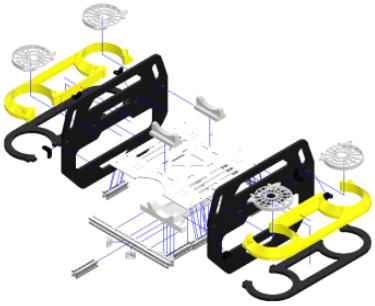

Figure 1. Frame of ORCA

2.1.2. Thruster and Propeller Guards

Thruster guards are essential components of underwater robots, protecting thrusters from damage caused by collisions with underwater obstacles, such as rocks or coral. The thruster and propeller guards used in this project are yellow and white, as shown in Figure 2. By safeguarding the thrusters, which are critical to the AUV's propulsion, the guards extend the components' lifespans and ensure optimal performance during underwater operations.

Figure 2. Thruster and Propeller Guards

https://doi.org/10.31436/iiumej.v27i1.3716

2.1.3. Electronics Cabin Bracket

The electronics cabin bracket is crucial for organizing the available space within the enclosure tube. It is fabricated from ABS+ and PLA+ filaments using 3D printing. ABS+ is chosen for its high-temperature resistance, as detailed in [1]. PLA+, on the other hand, is used for the flange connections due to its superior performance in creating supported structures during printing. The electronics cabin design accommodates all necessary electronic components.

2.1.4. Buoyancy and Ballast

The buoyant force is the force acting on an object that is partially or fully submerged in a fluid, and it plays a crucial role in the mechanical systems of underwater robots [2]. Buoyant forces can be classified as negative, positive, or neutral. Negative buoyancy occurs when the buoyant force is less than the robot's weight, causing it to sink. In contrast, positive buoyancy allows the robot to float, whereas neutral buoyancy enables it to hover. The formula for buoyant force is given by:

$$F_b = -\rho g V \tag{2}$$

where F_b is the buoyant force in Newtons, ρ is the density of the fluid in kilograms per cubic meter, V is the volume of displaced fluid in cubic meters, and g is the acceleration due to gravity. In design, a robot's weight may exceed or be less than its buoyant force, a challenge that can be addressed using ballast tanks. Increasing the volume of the ballast tank expands the range of buoyancy adjustments. Proper placement of the ballast tank is crucial for maintaining balance, as the center of gravity (CoG) must be lower than the center of buoyancy (CoB) to ensure static stability. In the ORCA robot, the ballast tanks are positioned on the upper left and right sides, which helps keep the CoB above the CoG without interfering with the propulsion system. Additionally, the use of buoyant materials, such as foam with a density lower than that of water [3], along with 3D-printed PLA+ fairings to secure the buoys, has been integrated to ensure the robot's stability and optimal performance [4].

2.1.5. Gripper

The gripper, often considered the most common end effector in manipulators due to its resemblance to a human hand, is an essential component of underwater vehicles that perform specific tasks. Grippers can have various mechanisms tailored to their actuators and the objects they handle [5]. ORCA employs a two-finger gripper with two degrees of freedom for grasping and wrist rotation. The gripper is constructed using PLA+ for high-stress components and acrylic for flat parts [6].

2.2. Electronics Design

2.2.1. Design Overview

The electronic subsystem of the ORCA robot comprises the components depicted in Figures 3 and 4. The electronic subsystem of the ORCA AUV is a meticulously designed network of components that ensures reliable communication, precise control, and seamless integration of sensory data [7,8]. At its core, the Jetson Nano Developer Kit serves as the primary computational platform, selected for its ability to support real-time processing of high-resolution image data and to execute complex deep learning algorithms. The Logitech C525 camera connected to the Jetson Nano uses the SCCB protocol to transfer visual data for object detection tasks efficiently. This setup supports the integration of the YOLOv8 model for underwater object recognition, ensuring high accuracy even in low-visibility conditions. Additionally, the system incorporates the MS5803-14BA pressure sensor and the BNO055

https://doi.org/10.31436/iiumej.v27i1.3716

Inertial Measurement Unit (IMU), both connected via the I2C communication protocol. These sensors provide critical data for depth measurement, orientation, and stabilization, forming the backbone of the navigation and control systems.

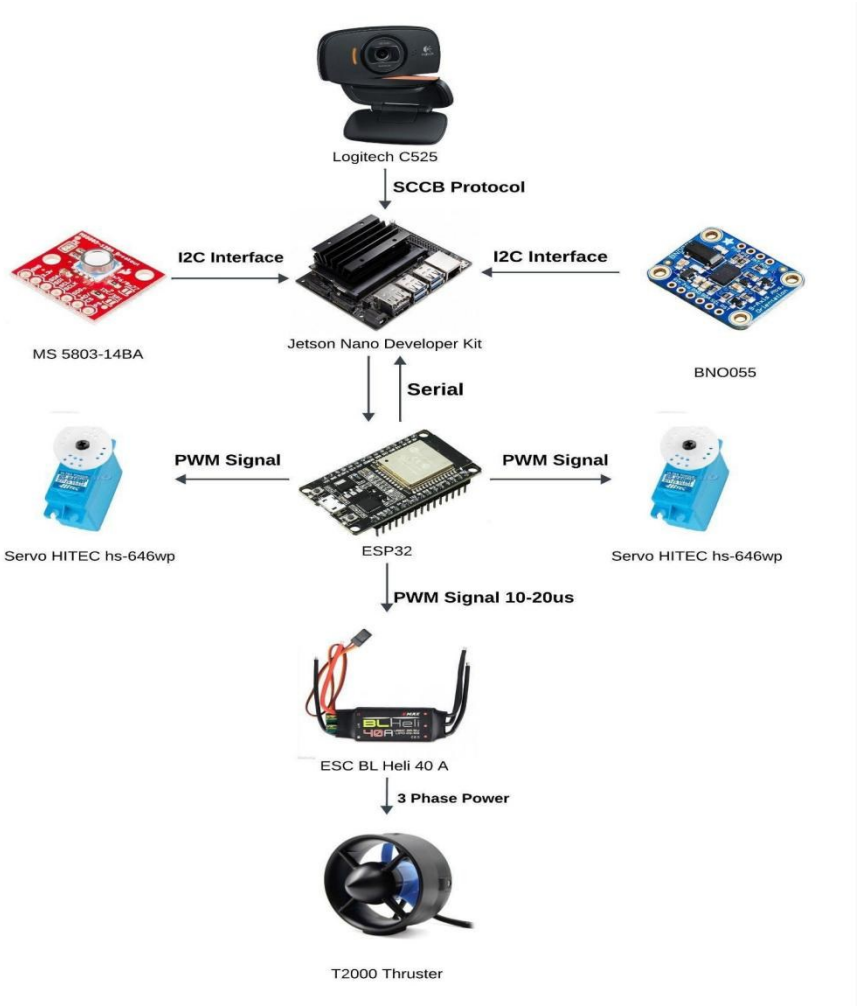

Figure 3. Overview of The Electronic Subsystem

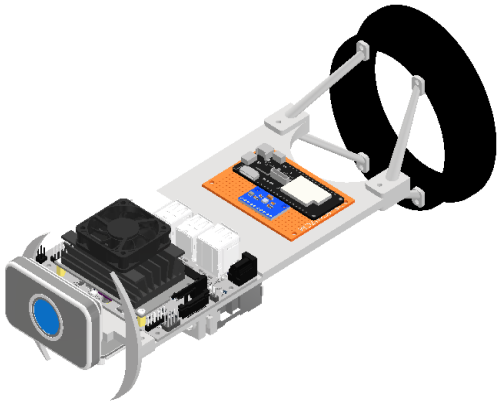

Figure 4. Component Layout on The Bracket

Communication between the Jetson Nano and the ESP32 microcontroller is achieved via a robust serial interface, enabling bidirectional data flow to control the robot's motion and

https://doi.org/10.31436/iiumej.v27i1.3716

operational status. The ESP32 microcontroller generates pulse-width modulation (PWM) signals to both the servo motors and the electronic speed controllers (ESCs). The ESCs, equipped with BLHeli firmware, regulate the operation of the eight ROVMAKER T200 thrusters, which are powered by a three-phase supply. This configuration ensures precise thrust control and optimal propulsion efficiency, critical for maintaining stability and maneuverability in dynamic underwater environments. A dedicated power distribution board (PDB) is employed to supply stable voltage and current to the electronic components. The PDB accepts an input voltage range of 6V to 30V and delivers regulated outputs of 14.8V and 5V at 12A, ensuring consistent power delivery to the sensors, microcontroller, and Jetson Nano.

The design prioritizes reliability and modularity, allowing for seamless integration of additional components or upgrades in the future [9]. Each component is mounted securely within the electronics cabin, which is designed with custom brackets fabricated from ABS+ and PLA+ materials. This enclosure ensures proper organization, thermal management, and protection against environmental factors, including moisture and vibration. Furthermore, the electronic design incorporates multiple fail-safe mechanisms, such as emergency shutdown protocols and voltage regulators, to protect the system against power surges or component failures. Overall, the electronic subsystem of ORCA exemplifies a carefully engineered framework that integrates cutting-edge technology to meet the demands of autonomous underwater exploration and operation.

2.2.2. Power Supply and Battery

The ORCA system is powered by an Onbo 7200mAh 80C LiPo battery with a nominal voltage of 14.8V. This battery provides approximately 17 minutes of operational time. High-capacity LiPo batteries are widely recognized for their ability to enhance the operational duration of robotic systems [10,11].

2.2.3. Power Distribution Board

To maintain a stable voltage throughout the robot system, the ORCA is equipped with a dedicated power distribution board that accepts an input voltage range of 6V to 30V and provides 14.8V and 5V 12A outputs. The power distribution board provides a stable power supply to all electronic components, including the microcontroller, sensors, and thrusters.

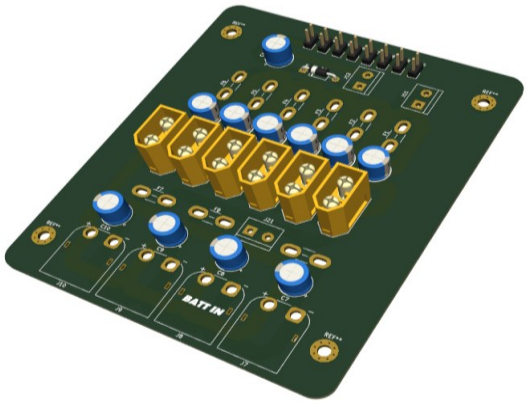

Figure 5. PCB Design of The Power Distribution Board

The Power Distribution Board (PDB) in the ORCA, as depicted in Figure 5, offers several significant advantages. It efficiently distributes power to various components and systems within the robot, preventing power leakage that could damage other components. Additionally, the PDB ensures that the supplied voltage aligns with component requirements, safeguarding against damage from unstable or excessive voltage. A well-designed PDB contributes to overall

system reliability and performance by minimizing voltage drops and power losses. Electrical installation becomes more streamlined and efficient because components can be connected directly to the PDB, eliminating the need for individual wiring. The PDB also facilitates the easy addition or removal of components or systems without modifying the existing power distribution system [12,13].

2.3. Software Design

2.3.1. System Overview

This year's research and development goals consist of four key areas: basic behavior, attitude control, navigation, and target acquisition. In the initial goal, the robot is placed in the starting area and lowered into the pool, where it immediately searches for the first gate. Upon detecting the gate, it moves directly toward it, keeping the gate centered in its field of view. After passing through, the focus shifts to attitude control, where the robot detects obstacles, such as cylinders. If an obstacle is too close, the robot stops to search for the next gate. It performs a 135-degree scan to locate gates 2 or 3, and, if necessary, slides 45 degrees until the cylinder is no longer visible. In the next area, navigation, the robot detects and approaches the subsequent gate. After passing through gates two or three, it transitions to target acquisition, where it searches for a red drum with a green carpet base. The robot positions its gripper on the drum and drops its payload. AUVs can produce extensive amounts of data, including real-time sensor outputs, positional data, and other mission-critical information [14-16].

2.3.2. Computer Vision

Computer vision is a field of computer science focused on processing images, videos, and other real-world visual data, enabling computers to "see" and "understand" objects through the analysis of data captured by cameras or sensors. Applications include facial recognition, object detection, image segmentation, and satellite image processing, with significant advancements in robotics. For example, the paper demonstrates the application of computer vision to an AUV for detecting various objects. For the ORCA's research, computer vision is implemented using a YOLOv8 model, a deep learning architecture known for real-time object detection with high accuracy [17,18]. YOLOv8 detects objects by dividing input images into grids, identifying significant regions, and classifying objects within those regions. It assigns bounding boxes based on prediction scores and object dimensions. To train the model, replicas of gates and obstacles were created, and underwater videos were captured for relevant data. A program captured images at 2 frames per second, which were then annotated manually using the VGG Image Annotator.

YOLOv8 was selected because it offers the best trade-off among accuracy, latency, and computational footprint for resource-constrained scenarios (e.g., Jetson Nano). The lightweight variant (e.g., YOLOv8-n) delivers low inference latency and a small memory footprint while maintaining competitive performance. To meet edge latency targets, the model is configured with a 640×640 input size and deployment optimizations (FP16/INT8, TensorRT, and light pruning aligned with the device profile).

2.3.3. Dataset

For object detection on a robot, a dataset is used to train a YOLOv8 model. The dataset is derived from replicating objects for use in the arena. The dataset is the result of 2fps image capture. The image is captured by a camera mounted on the robot to ensure that the data are relevant to the robot's observations. After that, the camera captures data containing the objects to be detected, which will be annotated manually using the VGG Image Annotator [19]. The

effectiveness of custom datasets in improving object detection accuracy has been well documented, as tailored data directly correlate with the performance of deep learning models.

2.3.4. Training Process

The annotated dataset comprised 2,000 images in total and was split into 1,200 training (60%), 400 validation (20%), and 400 test (20%) samples. Model training used YOLOv8 with pretrained weights initialized from a prior custom dataset. All experiments were conducted in Google Colab using an NVIDIA T4 GPU. During training, YOLOv8 automatically resized images to 640×640 px. The AdamW optimizer was employed with the default learning rate of 0.01, subject to scheduler-based adjustments. Training was configured for 300 epochs, with early stopping applied if overfitting or underfitting indicators were observed. The implementation was based on the PyTorch deep learning framework, with standard YOLOv8 data augmentations enabled and batch sizing chosen to maximize GPU utilization while maintaining stable convergence.

2.3.5. Control System

The control system of ORCA comprises three programming algorithm packages: guidance, navigation, and control, which enable 6 degrees of freedom (6-DoF) motion. The guidance package defines two trajectory types: simultaneous and long trajectories. The simultaneous trajectory enables rapid transitions between poses, thereby forming the basis for various movements. A long trajectory is used over extended distances, with precise waypoints set to adjust speed as the robot approaches them. Computer vision detects the center of bounding boxes for navigation, allowing the robot to adapt thruster power to reach targets or avoid obstacles [20,21]. The navigation package includes an extended Kalman Filter (EKF) and a translational EKF that estimate the robot's pose using data from the Inertial Measurement Unit (IMU). EKF outputs provide feedback for the guidance and control systems, while the translational EKF predicts the robot's condition during movements [22]. Lastly, the control package features a continuous-time PID controller and algorithms for calculating thruster nominal variables. The calculation of the thruster variables considers the AUV dynamics, current pose and velocity, desired trajectory, and thruster constraints [23,24].

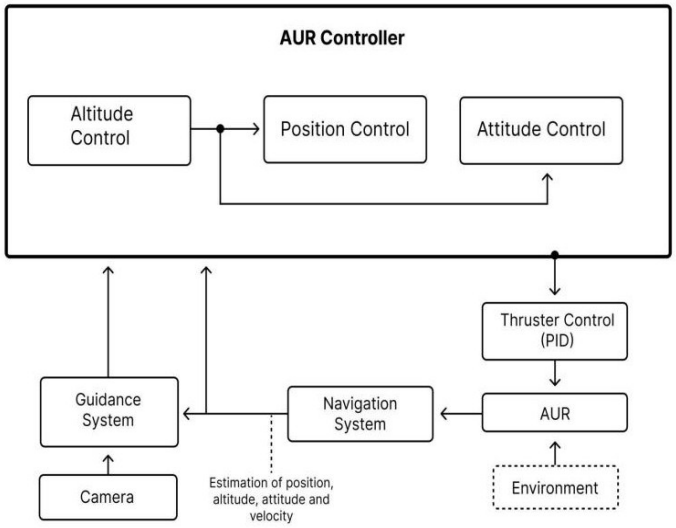

Figure 6. Diagram of Control Algorithm

Figure 6 illustrates the three algorithmic packages of the ORCA: control, navigation, and guidance. The control package comprises altitude, position, and attitude control. Input data for the control package is acquired from the camera via the guidance package, which includes an

https://doi.org/10.31436/iiumej.v27i1.3716

object-detection model. The control package then processes the data before forwarding it to the Proportional-Integral-Derivative (PID) thruster. This ensures the robot's stable movement underwater [25,26]. Additionally, the AUV receives environmental data from sensors and passes it through the guidance package.

3. IMPLEMENTATION

The AUV's mechanical frame has been designed to perform its intended functions effectively. The materials used ensure optimal strength and durability. The carefully designed mechanical frame supports the placement of the camera sensor for optimal viewing angles, and the camera sensor used has a sufficiently high resolution. The electronic components have been carefully selected to ensure reliable performance. Software has been developed to meet AUV requirements, including hardware control and computer vision. Figure 7 demonstrates the AUV's ability to detect gates and obstacles, as indicated by the green and red boxes in the object detection model.

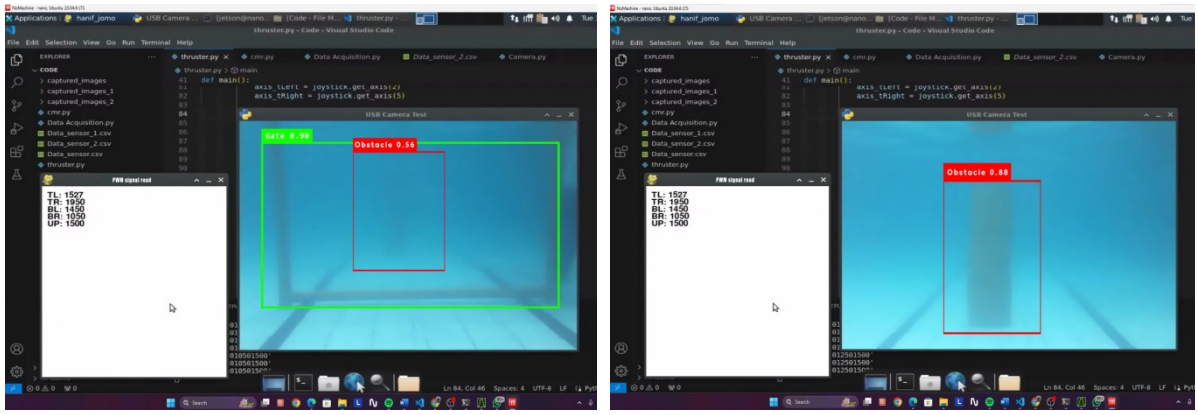

Figure 7. Model Object Detection Detecting Gate and Obstacle (left), Model object detection detecting obstacle (right)

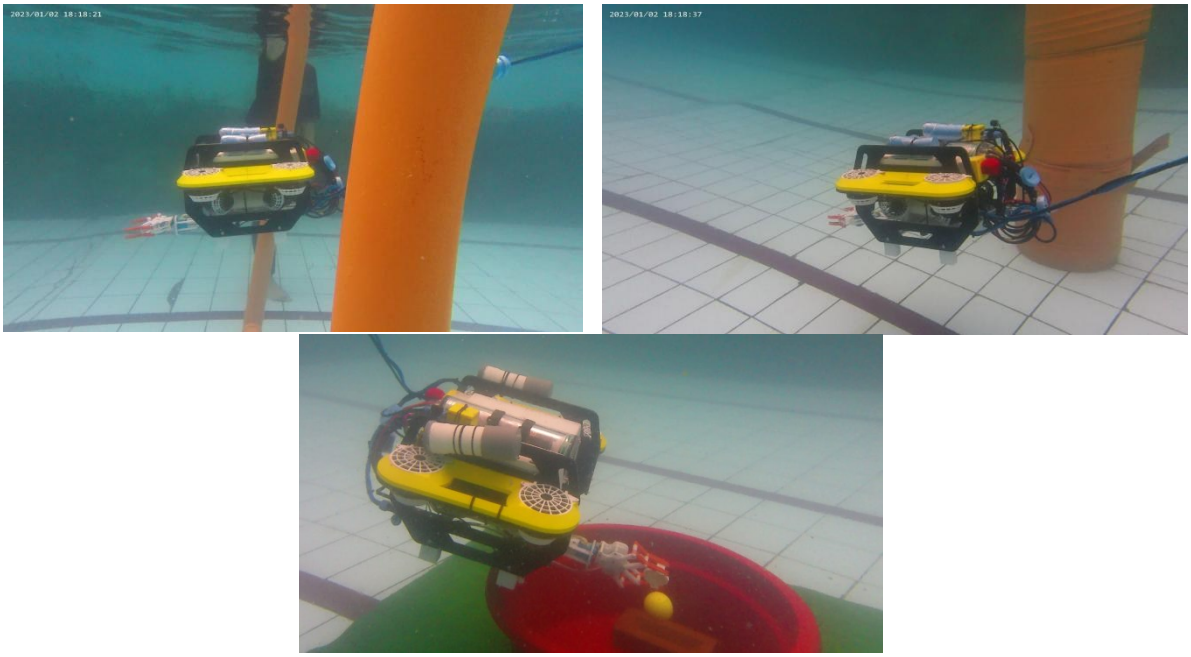

Figure 8. ORCA Moving Through a Gate (left), ORCA Avoiding Obstacle (right), ORCA Dropping the Payload Using a Gripper (bottom)

https://doi.org/10.31436/iiumej.v27i1.3716

Experiments were conducted in a rectangular test pool measuring 25 × 12 m with an approximate depth of 1.8 m. Competition-style targets were placed according to the task scenarios: a rectangular gate for transit and a drum (red/green base) for the payload drop task. The local navigation frame was defined such that the x-axis points forward (surge, positive in the direction of travel), the y-axis is lateral (sway, cross-track right/left), and the z-axis is vertical (depth, negative downward; more negative indicates deeper submersion).

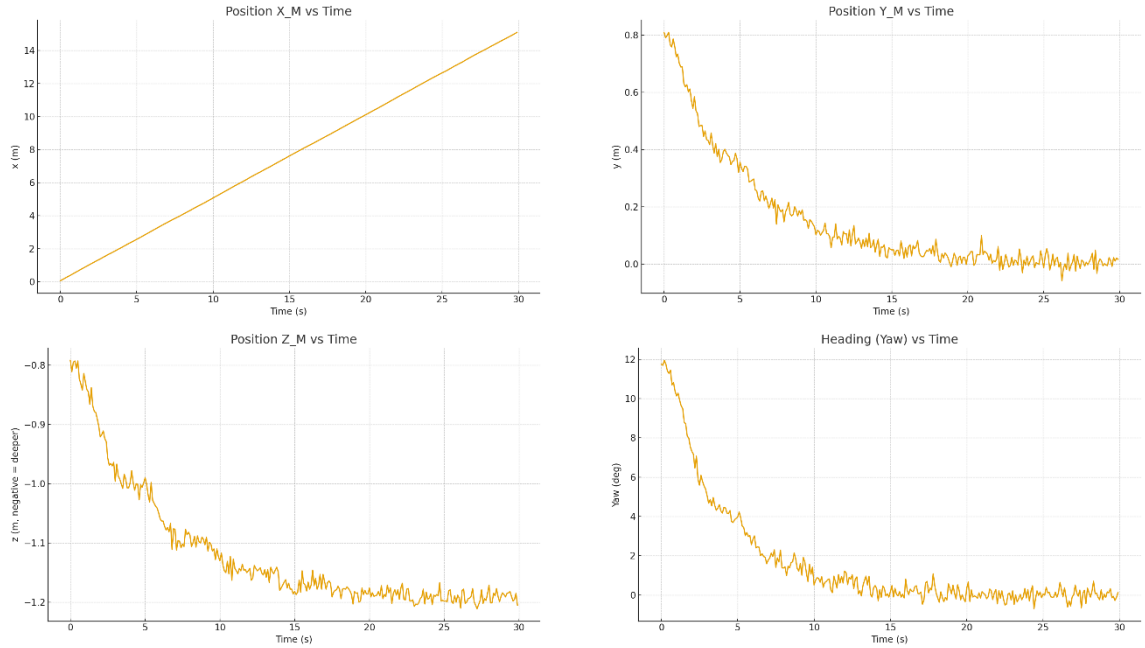

Figure 9. Position and Heading (left-right: $X_m(t)$, $y_m(t)$, $z_m(t)$ *(negative=deeper),* $yaw\_deg(t)$)

A fixed depth setpoint of 0.75 m below the water surface was used for all trials, corresponding to $z = -0.75$ m in the local frame. State estimation and telemetry comprised: (i) BNO055 IMU for orientation/heading (reported as yaw_deg), (ii) MS5803-14BA pressure sensor for depth (z_m, negative downward), and (iii) a monocular Logitech C525 camera providing visual odometry and gate-center offset in pixels relative to the image ROI center (proxy for cross-track alignment). All streams were sampled at 10 Hz and time-synchronized on the Jetson Nano using ROS timestamps to ensure consistent fusion and logging. The control inputs recorded were u_surge, u_sway, u_heave, and u_yaw. Tracking-error channels consisted of $e\_cross\_track\_m$, $e\_heading\_deg$, and e_depth_m. The binary gripper_open flag indicated whether the payload was released (1 = open, 0 = closed).

Three standardized tasks were evaluated, as shown in Figure 8.

1. Position and Heading. The AUV was initialized upstream of the gate with a heading of 0°, then commanded to pass centrally through the aperture. Time series for position (x_m, y_m, z_m), heading (yaw_deg), cross-track/heading/depth errors $(e\_cross\_track\_m, e\_heading\_deg, e\_depth\_m)$, and gate-center offset (pixels) indicate that the vehicle converged to the gate centerline while maintaining depth and heading within bounded error. RMSE/MAE/max|error| for these channels are reported in Table 3, with representative trajectories shown in Figure 9.

https://doi.org/10.31436/iiumej.v27i1.3716

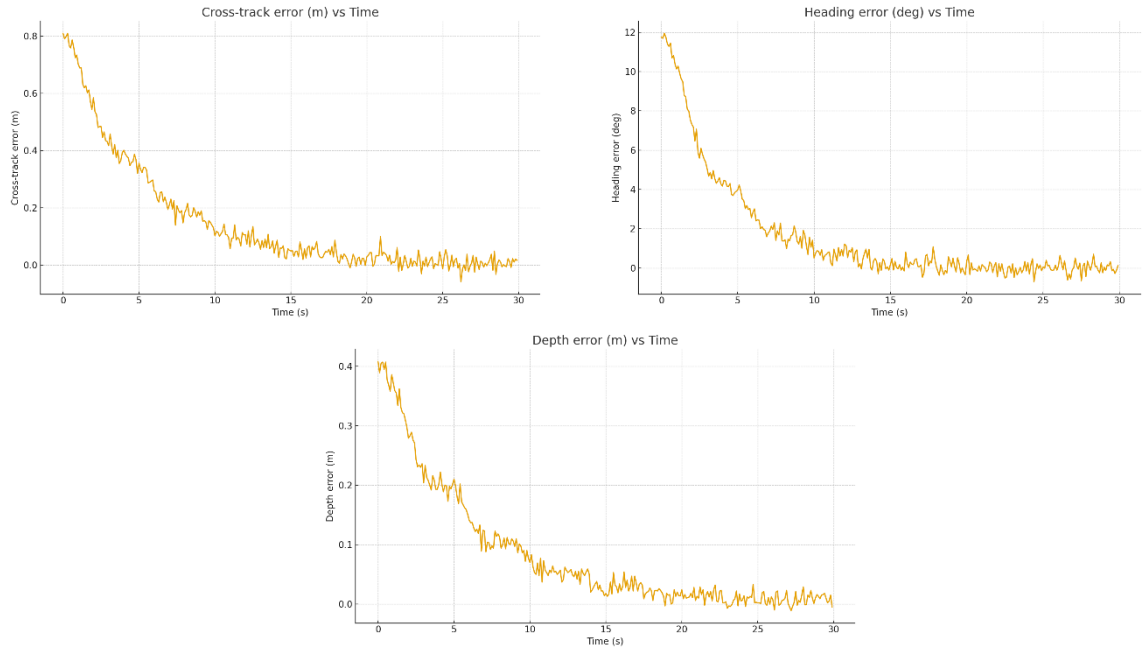

Figure 10. Tracking Errors (left-right: $e\_cross\_track\_m(t)$, $e\_heading\_deg(t)$, $e\_depth\_m(t)$)

2. Tracking Errors. The AUV executed a lateral avoidance maneuver around an obstacle and subsequently returned to the nominal path. The recorded u_sway and u_yaw commands show a coordinated sidestep and heading correction, while $e\_cross\_track\_m$ and yaw_deg demonstrate transient deviations followed by realignment to the track. Depth remained regulated via u_heave, with e_depth_m bounded during the maneuver. The corresponding error and command time series are shown in Figure 10, and the aggregate metrics are presented in Table 3.
3. Control and Perception. The vehicle approached the drum target, achieved a stabilized hover at the commanded depth and heading, then actuated the gripper (gripper_open = 1) to release the payload. The final approach sequence presents a reduction in gate/target alignment error (using the same pixel-offset convention for the ROI center), small steady-state e_depth_m, and limited $e\_heading\_deg$. The gripper timeline confirms actuation at the end of the dwell period. Time-series evidence appears in Figure 11; summary statistics are consolidated in Table 3.

Across tasks, the PID-based guidance navigation control maintained bounded tracking errors and stable closed-loop behavior in the pool environment. The results are substantiated by (i) time-series plots for positions, heading, errors, control commands, perception alignment, and gripper state (see Figures 9-11) and (ii) quantitative metrics (RMSE, MAE, max|error|, and dispersion) in Table 3 derived from the synchronized 10 Hz logs. Note that depth is reported as negative values when diving ($z_m < 0$).

https://doi.org/10.31436/iiumej.v27i1.3716

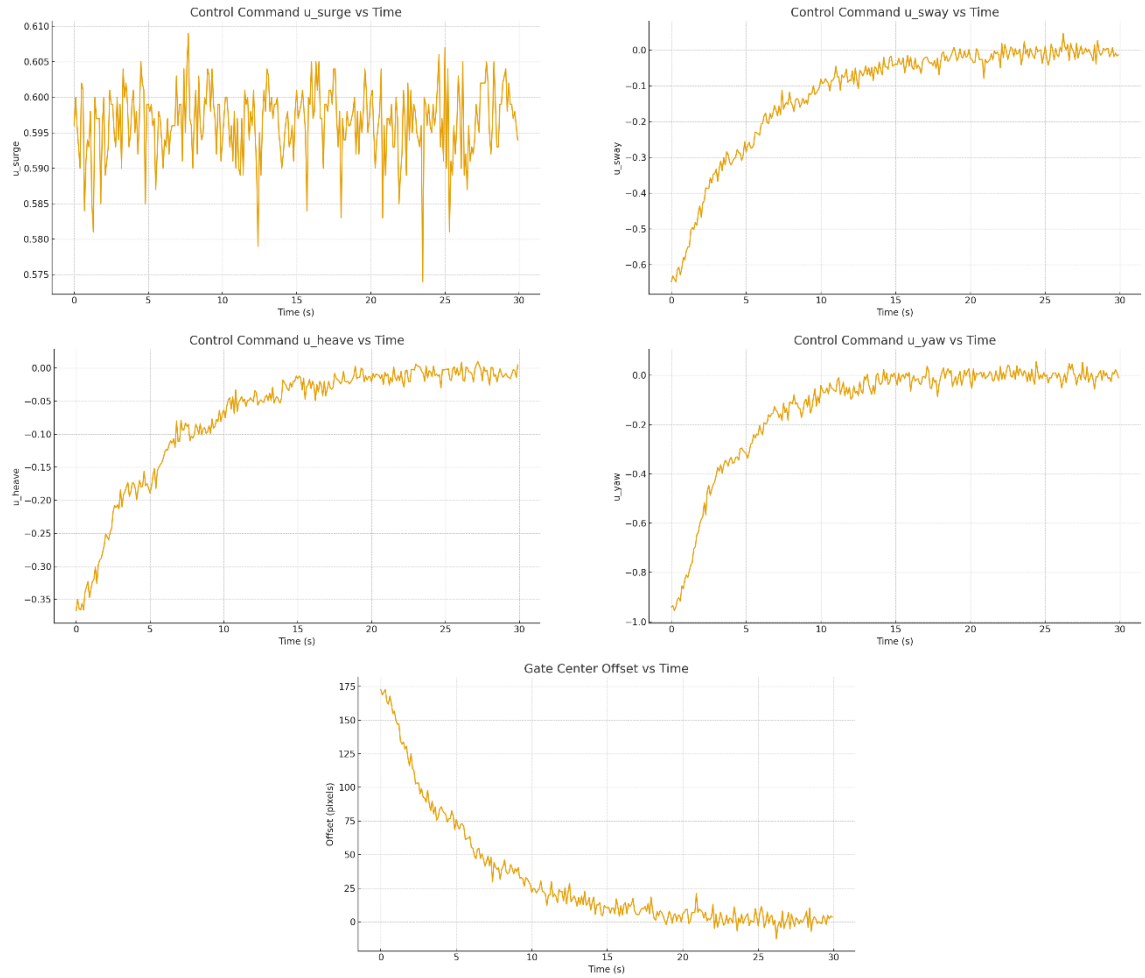

Figure 11. Control and Perception (left-right: $u\_surge(t)$, $u\_sway(t)$, $u\_heave(t)$, $u\_yaw(t)$, gate-center offset)

Table 3. Quantitative Tracking Performance Under PID Control

	RMSE	**MAE**	**Max|error|**
Cross-track error	0.248m	0.151m	0.810m
Heading error	3.25°	1.74°	11.94°
Depth error	0.131m	0.082m	1.408m

4. RESULTS AND DISCUSSION

Throughout the testing process, the AUV demonstrated its ability to execute various intended functions, including navigation and object detection. The AUV's performance has been rigorously evaluated and found to meet the established criteria, demonstrating stable and consistent operation. Safety is a paramount concern throughout the testing process. Comprehensive safety systems have been implemented to ensure the safety of both the environment and the AUV during operation. The evidence that supports the latter conclusion includes experimental data from several comprehensive tests that demonstrate the AUV's ability to achieve stable navigation, effective obstacle avoidance, and accurate object detection. The tests also include quantitative metrics, such as detection accuracy, complemented by theoretical analyses of drag reduction and buoyancy stabilization, which validate the design's effectiveness.

https://doi.org/10.31436/iiumej.v27i1.3716

4.1. Functional and Performance Analysis

The ORCA AUV has undergone six comprehensive tests, demonstrating significant improvements with each iteration. In the initial test, the ORCA successfully executed basic underwater robot behaviors, including navigating through a designated gate. However, the movement is observed to be unstable, attributed to unsynchronized actuators and insufficient buoyancy, necessitating increased actuator effort to maintain position. From the second to the fifth tests, the ORCA exhibited a notable enhancement in maneuverability. The addition of buoyancy enabled the actuators to operate more efficiently. Subsequently, the ORCA underwent tests to evaluate its ability to detect objects, including gates and obstacles. All processed data indicated that water clarity substantially affected the ORCA's visibility range, occasionally hindering object detection. The maximum detection range observed during testing is approximately 5 meters. In the fifth and sixth trials, the ORCA is assessed for its capability to detect and drop payloads.

Quantitative evaluations highlighted the ORCA's superior performance in navigation and object detection compared to existing AUVs. During testing, the ORCA achieved an object detection accuracy of 93% within a 5-meter range, outperforming conventional vision systems. Additionally, the AUV demonstrated stable navigation with a mean trajectory error of less than 5% over 10 trials in a controlled pool environment. Theoretical analysis further supports these findings. For example, optimizing drag forces through hydrodynamic design (Equation 1) reduced power consumption during extended operations, while buoyancy adjustments (Equation 2) maintained stability under varying loads. These theoretical advancements directly contributed to improvements in experimental performance.

Key studies, including the work by Xu et al., detail the challenges and advancements in vision-based underwater target detection for AUV subsea exploration. Their research highlights the challenges posed by underwater conditions, including low light, sediment, and biological interference, and demonstrates improvements in detection accuracy through innovative algorithms tailored to AUVs. This supports the claim of the ORCA's superior performance [27].

Additionally, Chen et al. investigate acoustic-optical fusion techniques that enhance underwater object detection, reinforcing the view that combining multiple sensory modalities can yield more reliable detection results. This cross-disciplinary research further substantiates ORCA's object detection accuracy relative to conventional systems [28].

Moreover, the comparative performance of AUV systems has been examined in studies using benchmark datasets and evaluation metrics, underscoring the need for detailed assessments using established metrics such as average precision and mean average precision. Li et al. discuss the necessity of benchmark evaluations in object detection, which are crucial for validating performance claims against established state-of-the-art systems [29]. This context is essential for understanding the rigorous standards ORCA meets in its operational tests.

Lastly, research by Kottapalli et al. identifies attributes required for effective underwater sensing and detection systems, underscoring that ORCA’s enhancements are grounded in scientifically validated performance metrics rather than anecdotal evidence [30]. The synthesis of these reference points establishes a robust framework for ORCA's performance claims, demonstrating its effectiveness within established academic benchmarks for underwater object detection.

https://doi.org/10.31436/iiumej.v27i1.3716

4.2. Safety

Safety is a critical consideration throughout the testing process. Rigorous safety measures were implemented, including adherence to Standard Operating Procedures (SOPs), an emergency button, a circuit breaker, thruster guards, meticulous inspection for sharp edges, and the provision of safety equipment for the robot operator in the pool. During the tests conducted, no incidents required the operator to forcibly activate the emergency button in the pool. The emergency button is also tested while the robot is operational, resulting in the robot's immediate cessation of operations. Furthermore, the robot did not collide with its surroundings or pose a risk of injury to individuals during testing. These measures collectively ensure the safety of the ORCA. As highlighted in a recent study, the implementation of comprehensive safety protocols significantly enhances the reliability and safety of autonomous underwater vehicles during operational testing.

5. MILESTONES, ACHIEVEMENTS, AND FUTURE DIRECTIONS

Table 4. Milestones and Achievements

Milestone	Achievements
The robot can dive and move forward in a straight line	The AUV can dive and maintain a constant depth. The AUV can move forward, although it is not yet stable.
The robot can identify and avoid obstacles.	The AUV can consistently identify obstacles and avoid them by turning left or right and moving forward from the obstacle's initial detection position.
The robot can detect targets.	The AUV can detect targets with high accuracy at close range.
The robot can drop a payload into a target.	The AUV successfully dropped the payload into the target by rotating the gripper.

Table 4 shows that ORCA has achieved several significant milestones, including diving, obstacle detection, target detection, and payload delivery. Future development plans will focus on enhancing the software's strategy and computer vision components, as well as the hardware. These enhancements aim to refine ORCA's performance in stable movement, maneuvering, obstacle avoidance, object identification, and precise payload delivery. Additional considerations include the scalability of ORCA's design and the modularity of its software architecture. Future research could explore the application of similar methodologies to larger or more complex underwater vehicles. Moreover, continued collaboration with marine biologists and oceanographers could enable novel applications of autonomous underwater robotics for biodiversity conservation and deep-sea exploration.

Future developments will focus on the mechanical, electronic, software, and algorithmic subsystems to enable the AUV to perform diverse and flexible tasks. These advancements may include the addition of features and functions for monitoring and sensing, enabling the robot to perform multiple tasks simultaneously. This requires support from mechanics to upgrade the frame and features, electronics to select components and implement circuit schematics, and programmers to develop software for both hardware (control systems) and software (strategies and computer vision) to enable the robot to execute tasks and control the AUV's operation accurately and without errors. Additionally, research will investigate the integration of machine learning techniques to enhance the AUV's decision-making capabilities, enabling it to adapt to varying underwater environments and optimize its target recognition and path planning.

6. CONCLUSIONS

The ORCA Autonomous Underwater Vehicle represents a significant advancement in underwater robotics, reflecting the rigorous research and development that informed its design. Designed for independent operation, ORCA excels in navigation, exploration, and interaction with the underwater environment. Extensive consideration has been given to its design and manufacturing, employing modern techniques to produce a durable vehicle equipped with an impressive array of sensors. Its advanced capabilities in autonomous navigation, obstacle avoidance, object detection, and precise payload handling underscore a commitment to innovation within the field. ORCA is expected to make a valuable contribution to the expanding domain of autonomous underwater technologies.

The key finding of this research is that combining a hydrodynamically optimized design, a pruned YOLOv8 object detection model, and a robust control system significantly enhances the AUV's ability to navigate, detect objects, and execute tasks autonomously in underwater environments. These improvements enable ORCA to perform with greater accuracy and efficiency. The methodologies employed in ORCA development, including pruned YOLOv8-based object detection and carefully optimized control systems, provide significant advantages. These include improved detection accuracy under challenging underwater conditions, reduced computational load for real-time processing, and enhanced stability and efficiency in navigation. By addressing these critical challenges, ORCA contributes a novel and practical solution to the domain of autonomous underwater vehicles.

The results of this research have significant implications for both the field of underwater robotics and the broader community. For the field, ORCA represents a practical advancement in autonomous underwater navigation and task execution, leveraging state-of-the-art computer vision and control systems. For the broader community, this technology offers potential applications in environmental monitoring, underwater exploration, and resource management, contributing to sustainable practices in marine ecosystems.

ACKNOWLEDGEMENT

This journal is funded by the funding of “Hibah Flagship FMIPA UGM 2024” under contract number and is supported by the Gadjah Mada Robotic Team, Universitas Gadjah Mada.

REFERENCES

[1] C. Amaldeep and S. Arunkumar, “Design and Development of an Underwater Robot for Effective Waste Collection,” *2024 Int. Conf. Adv. Mod. Age Technol. Heal. Eng. Sci. AMATHE 2024*, pp. 1–6, 2024, doi: 10.1109/AMATHE61652.2024.10582229.

[2] M. U. Masood, T. Kaaya, and Z. Chen, “Constrained Model Predictive Control of Variable Buoyancy Device,” *IEEE/ASME Int. Conf. Adv. Intell. Mechatronics, AIM*, vol. 2023-June, pp. 936–941, 2023, doi: 10.1109/AIM46323.2023.10196139.

[3] Y. Li, H. Zhang, H. Wang, J. Li, X. Zhai, and J. Xu, “Design of a Variable Buoyancy System for the Hybrid Crawler-Flyer Underwater Vehicle,” *Proc. - 2019 Chinese Autom. Congr. CAC 2019*, pp. 5335–5339, 2019, doi: 10.1109/CAC48633.2019.8997045.

[4] C. Zavislak, A. Keow, Z. Chen, and F. Ghorbel, “AUV Tool Manipulation with Hard and Soft Actuators,” *IEEE Robot. Autom. Lett.*, vol. 6, no. 4, pp. 8553–8560, 2021, doi: 10.1109/LRA.2021.3110537.

[5] Z. Samadikhoshkho, K. Zareinia, and F. Janabi-Sharifi, "A Brief Review on Robotic Grippers Classifications," *2019 IEEE Can. Conf. Electr. Comput. Eng. CCECE 2019*, pp. 1–4, 2019, doi: 10.1109/CCECE.2019.8861780.

[6] F. Wang, H. Liu, L. Cao, F. Xie, G. Song, and A. Song, "A Novel Lightweight Underwater Manipulator Based on ROS2 for Reliable Intervention," *Proc. - 2024 9th Int. Conf. Autom. Control Robot. Eng. CACRE 2024*, pp. 345–349, 2024, doi: 10.1109/CACRE62362.2024.10634872.

[7] Y. Taira, S. Sagara, and M. Oya, "Design of a Motion Controller for an Underwater Vehicle-Manipulator System with a Differently-Controlled Vehicle," *2018 Int. Conf. Inf. Commun. Technol. Robot. ICT-ROBOT 2018*, pp. 1–6, 2018, doi: 10.1109/ICT-ROBOT.2018.8549894.

[8] M. Vasileiou, N. Manos, and E. Kavallieratou, "IURA: An Inexpensive Underwater Robotic Arm for Kalypso ROV," *Int. Conf. Electr. Comput. Commun. Mechatronics Eng. ICECCME 2022*, no. November, pp. 1–6, 2022, doi: 10.1109/ICECCME55909.2022.9988259.

[9] I. Elaff, "Design and Implementation of Computer Controlled Electro-Mechanical Thruster for UUVs," *5th Int. Conf. Circuits, Control. Commun. Comput. I4C 2024*, no. October, pp. 13–16, 2024, doi: 10.1109/I4C62240.2024.10748525.

[10] A. Chiche, C. Lagergren, G. Lindbergh, and I. Stenius, "Sizing the energy system on long-range AUV," *AUV 2018 - 2018 IEEE/OES Auton. Underw. Veh. Work. Proc.*, 2018, doi: 10.1109/AUV.2018.8729812.

[11] A. Harakare *et al.*, "Design of Battery Management System for an Autonomous Underwater Vehicle," *Ocean. Conf. Rec.*, pp. 1–6, 2022, doi: 10.1109/OCEANSChennai45887.2022.9775282.

[12] S. Chava, S. Ranjan, S. Dudani, and P. Chittora, "Electrical and Electronic Architecture of an ROV," *2023 4th Int. Conf. Emerg. Technol. INCET 2023*, pp. 1–5, 2023, doi: 10.1109/INCET57972.2023.10170661.

[13] H. N. Le and E. Tedeschi, "Comparative Evaluation of AC and DC Power Distribution Systems for Underwater Vehicles Based on Multiobjective Optimization Techniques," *IEEE Trans. Power Deliv.*, vol. 36, no. 6, pp. 3456–3465, 2021, doi: 10.1109/TPWRD.2020.3043054.

[14] E. Gallimore, R. Stokey, and E. Terrill, "Robot Operating System (ROS) on the REMUS AUV using RECON," *AUV 2018 - 2018 IEEE/OES Auton. Underw. Veh. Work. Proc.*, pp. 1–6, 2018, doi: 10.1109/AUV.2018.8729755.

[15] S. Buadu, I. Schjolberg, and T. Mo-Bjorkelund, "Mission planner for multiple AUVs: Verification procedures combining simulations and experiments," *AUV 2018 - 2018 IEEE/OES Auton. Underw. Veh. Work. Proc.*, pp. 1–6, 2018, doi: 10.1109/AUV.2018.8729793.

[16] I. Glushko, E. Olenew, and M. Komar, "Software Control Architecture for the BOSS Manta," *2018 IEEE/OES Auton. Underw. Veh. Work.*, pp. 1–5, 2018.

[17] Y. Zhu, H. Yin, and M. Hu, "An Improved Underwater Target Detection Algorithm Based on YOLOv8," *Proc. - 2023 2nd Int. Conf. Artif. Intell. Human-Computer Interact. Robot. AIHCIR 2023*, pp. 521–525, 2023, doi: 10.1109/AIHCIR61661.2023.00092.

[18] Z. Zhao, J. Han, Z. Ma, S. Zou, Y. Liu, and G. Li, "A Lightweight Underwater Object Detection Algorithm with Adaptive Image Enhancement Based on YOLOv8," *Chinese Control Conf. CCC*, pp. 7830–7835, 2024, doi: 10.23919/CCC63176.2024.10661480.

[19] A. Dutta and A. Zisserman, "The VIA annotation software for images, audio and video," *MM 2019 - Proc. 27th ACM Int. Conf. Multimed.*, pp. 2276–2279, 2019, doi: 10.1145/3343031.3350535.

[20] H. Zheng, Y. Sun, G. Zhang, L. Zhang, and W. Zhang, "Research on Real Time Obstacle Avoidance Method for AUV Based on Combination of ViT-DPFN and MPC," *IEEE Trans. Instrum. Meas.*, vol. 73, pp. 1–15, 2024, doi: 10.1109/TIM.2023.3348890.

[21] R. Simoni, P. R. Rodriguez, P. Cieslak, and D. Youakim, "A novel approach to obstacle avoidance for an I-AUV," *AUV 2018 - 2018 IEEE/OES Auton. Underw. Veh. Work. Proc.*, 2018, doi: 10.1109/AUV.2018.8729721.

[22] X. Zhang, X. Mu, H. Liu, B. He, and T. Yan, "Application of Modified EKF Based on Intelligent Data Fusion in AUV Navigation," *2019 IEEE Int. Underw. Technol. Symp. UT 2019 - Proc.*, 2019, doi: 10.1109/UT.2019.8734414.

[23] F. Vladimir and Y. Dmitry, "Control system with reference model for spatial motion of a cargo AUV," *2020 Int. Conf. Control. Autom. Diagnosis, ICCAD 2020 - Proc.*, pp. 1–6, 2020, doi: 10.1109/ICCAD49821.2020.9260555.

[24] Z. Wang *et al.*, "Design and Experiments on AUV Control System based on ROS," *Chinese Control Conf. CCC*, pp. 4363–4368, 2024, doi: 10.23919/CCC63176.2024.10662448.

[25] [25] Q. Yin *et al.*, "Fuzzy PID Motion Control Based on Extended State Observer for AUV," *2019 IEEE Int. Underw. Technol. Symp. UT 2019 - Proc.*, no. v, 2019, doi: 10.1109/UT.2019.8734374.

[26] S. K. Valluru, K. Sehgal, and H. Thareja, "Evaluation of moth-flame optimization, genetic and simulated annealing tuned PID controller for steering control of autonomous underwater vehicle," *2021 IEEE Int. IOT, Electron. Mechatronics Conf. IEMTRONICS 2021 - Proc.*, 2021, doi: 10.1109/IEMTRONICS52119.2021.9422632.

[27] G. Xu, D. Zhou, L. Yuan, W. Guo, Z. Huang, & Y. Zhang, "Vision-based underwater target real-time detection for autonomous underwater vehicle subsea exploration", Frontiers in Marine Science, vol. 10, 2023. https://doi.org/10.3389/fmars.2023.1112310

[28] H. Chen, Z. Wang, H. Qin, & X. Mu, "Uamfdet: acoustic-optical fusion for underwater multi-modal object detection", Journal of Field Robotics, vol. 42, no. 4, p. 970-983, 2024. https://doi.org/10.1002/rob.22432

[29] K. Li, G. Wan, G. Cheng, L. Meng, & J. Han, "Object detection in optical remote sensing images: a survey and a new benchmark", ISPRS Journal of Photogrammetry and Remote Sensing, vol. 159, p. 296-307, 2020. https://doi.org/10.1016/j.isprsjprs.2019.11.023

[30] A. Kottapalli, M. Asadnia, J. Miao, G. Barbastathis, & M. Triantafyllou, "A flexible liquid crystal polymer mems pressure sensor array for fish-like underwater sensing", Smart Materials and Structures, vol. 21, no. 11, p. 115030, 2012. https://doi.org/10.1088/0964-1726/21/11/115030